



# Application of machine learning in fracture analysis of edge crack semi-infinite elastic plate

Saeed H. Moghtaderi\*

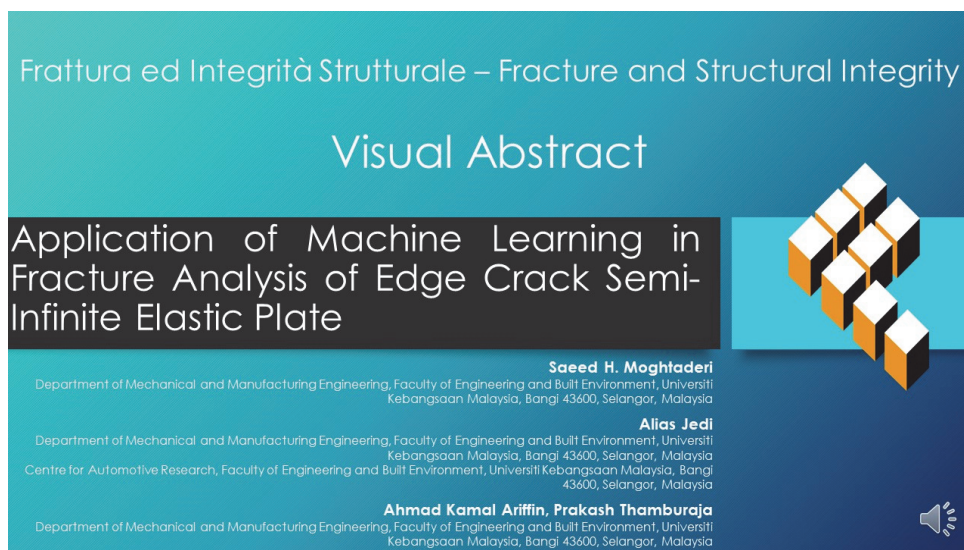
*Department of Mechanical and Manufacturing Engineering, Faculty of Engineering and Built Environment, Universiti Kebangsaan Malaysia, Bangi 43600, Selangor, Malaysia*  
*p116028@siswa.ukm.edu.my, <https://orcid.org/0000-0002-0047-9854>*

Alias Jedi

*Department of Mechanical and Manufacturing Engineering, Faculty of Engineering and Built Environment, Universiti Kebangsaan Malaysia, Bangi 43600, Selangor, Malaysia*  
*Centre for Automotive Research, Faculty of Engineering and Built Environment, Universiti Kebangsaan Malaysia, Bangi 43600, Selangor, Malaysia*  
*aliasjedi@ukm.edu.my, <https://orcid.org/0000-0002-2106-0542>*

Ahmad Kamal Ariffin, Prakash Thamburaja

*Department of Mechanical and Manufacturing Engineering, Faculty of Engineering and Built Environment, Universiti Kebangsaan Malaysia, Bangi 43600, Selangor, Malaysia*  
*kamal3@ukm.edu.my, <https://orcid.org/0000-0001-5098-5088>*  
*p.thamburaja@ukm.edu.my, <https://orcid.org/0000-0002-2639-6651>*



**Citation:** Moghtaderi, S. H., Jedi, A., Ariffin, A. K., Thamburaja, P., Application of machine learning in fracture analysis of edge crack semi-infinite elastic plate, *Frattura ed Integrità Strutturale*, 68 (2024) 197-208.

**Received:** 12.12.2023

**Accepted:** 31.01.2024

**Published:** 05.02.2024

**Issue:** 04.2024

**Copyright:** © 2024 This is an open access article under the terms of the CC-BY 4.0, which permits unrestricted use, distribution, and reproduction in any medium, provided the original author and source are credited.

**KEYWORDS.** Mode I fracture analysis, Machine learning, Finite element analysis, Elastic plate, Stress intensity factor.



## INTRODUCTION

Understanding fatigue and fracture assessment of solid structures and materials such as beams [1,2], plates [3,4], and bars [5,6] is critical for guaranteeing their integrity and durability, as well as building safe and resilient engineering systems. Various analytical and computational approaches have been used throughout the years to analyze fracture propagation and stress distribution in such systems [7]. Among these techniques, the stress intensity factor (SIF) model has shown to be a basic tool for studying the stress field around crack tips, offering useful insights into solid component fracture mechanics [8,9]. The SIF model, which is widely used in mode I fracture analysis, has been facilitated by incorporating suitable intrinsic length scales, enabling researchers to describe size effect phenomena and determine critical conditions for crack propagation as well as evaluate the structural integrity of materials [10,11]. This model describes the stress concentration at the crack tip and is crucial in estimating the crack growth rate under various loading conditions.

Numerical simulation, on the other hand, has become an essential tool in engineering methodologies, offering an efficient means for investigating complex systems. The Finite Element Analysis (FEA) approach has gained significant acceptance in this context for investigating fracture behavior, aided by software tools such as ABAQUS CAE and ANSYS Workbench to perform extensive numerical simulations of fracture propagation in complex solid structures, resulting in a rich dataset that incorporates experimental data [12-14].

The application of machine learning (ML) techniques in fracture analysis has influenced the area of material engineering and structural mechanics in recent years [15,16]. ML approaches provide a data-driven technique to analyzing complicated fracture patterns, revealing important information about crack propagation, stress distribution, and failure processes [17,18]. These approaches are capable of handling massive datasets generated by numerical simulations and experimental findings in an effective way, allowing the construction of prediction models with outstanding precision [19,20].

Artificial Neural Network (ANN) is a popular machine learning (ML) technique in mode I fracture analysis. ANN is a flexible and effective technique that can learn complicated correlations and patterns from data. It is made up of intertwined layers of networks that analyze data and generate predictions. ANN can successfully capture the crack growth and stress distribution in the context of fracture analysis, making it appropriate for predicting essential crack lengths, fatigue life, and fracture toughness [21]. However, the data in fracture analysis can be complicated, with nonlinear correlations between multiple input variables, and classified inputs such as crack length and mesh type can introduce further complexity, resulting in less accurate predictions [22]. Such ML models not only accelerate fracture analysis processes, but also allow researchers to productively examine various design conditions, assisting in the optimization of engineering structures for improved reliability and efficiency [23-25].

The current study incorporates the stress intensity factor (SIF) model to evaluate the maximum normal stress distribution around the crack tip of a 2D edge-crack semi-infinite elastic plate. To accomplish such an objective, numerical simulations were performed using finite element analysis (FEA) with ABAQUS CAE, taking into account an extensive variety of crack lengths and mesh sizes. The numerical findings were then compared to the SIF model predictions for various crack lengths and characteristic length parameters. Following that, machine learning (ML) techniques, particularly artificial neural network (ANN) model, was used to categorize and develop an ML model based on the numerical simulation results. The crack length and simulation iterations have been employed as the input variables in this ML model, whereas the maximum normal stress in the crack line direction provided output. The accuracy of the ML model has been confirmed through the examination of testing data, specifically a subset of FEM results employed for model testing. The implementation details of the algorithms used for ML and Python programming can be discovered in the appendix. This study aims to get an in-depth comprehension of crack behavior in semi-infinite elastic plates and to give an efficient and accurate strategy for predicting stress distribution at the crack tip by combining the SIF model, numerical simulations, and ML approaches.

## STRESS INTENSITY FACTOR MODEL

Consider a two-dimensional model of an edge-crack semi-infinite elastic plate as shown in Fig. 1 which is under the tension of  $\sigma_0$  with the dimensions of  $w \times h$  and density, elasticity modulus, and Poisson ratio of  $\rho$ ,  $E$ , and  $\nu$ , respectively and a tip crack of length  $a$ . An edge-crack semi-infinite plate contains a crack length that is considerably smaller than the plate width ( $a/w \rightarrow 0$ ) and due to this geometric relationship, specific analytical and numerical methods, such as stress intensity factor modeling, are available to properly examine fracture behavior and its impact on overall structural integrity.

Linear Elastic Fracture Mechanics (LEFM) is a classic fracture mechanics theory that is indispensable in understanding crack propagation in brittle materials. LEFM introduced the SIF model, which builds on Griffith's theory, which establishes a link

between stress fields, crack length, and material properties in brittle materials like glass. The SIF model determines stress concentration at the crack tip and its link to crack growth. The SIF is an important parameter that assesses the mechanical force for crack propagation in materials with insignificant plastic deformation at the crack tip [26].

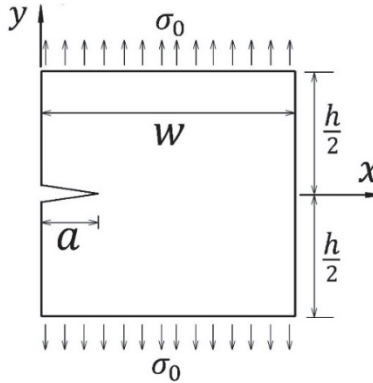


Figure 1: Schematic configuration of an edge-crack semi-infinite elastic plate.

A crack is depicted in Fig. 2 as a schematic illustration of a linear elastic isotropic two-dimensional plate. The region around the crack tip is designated by the coordinates  $r$  and  $\theta$ , and an arbitrary stress element is shown within this area.

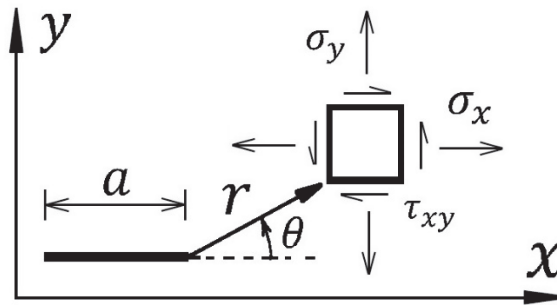


Figure 2: Stress components near the crack tip ( $r \ll a$ ).

Using the LEFM and Westergaard stress function in complex form, the stress component in the y-direction can be obtained by:

$$\sigma_y = \frac{K}{\sqrt{2\pi r}} \cos\left(\frac{\theta}{2}\right) \left(1 + \cos\left(\frac{\theta}{2}\right) \sin\left(3\frac{\theta}{2}\right)\right) \tag{1}$$

where  $K$  is the stress intensity factor, that is described as the elastic energy per unit crack surface area required for crack growth and is related to the energy release rate.  $K$  can be calculated analytically, computationally, or experimentally, and its relationship can be expressed as:

$$K = \beta \sigma_0 \sqrt{a} \tag{2}$$

where  $\beta$ ,  $\sigma_0$ , and  $a$  stand for the geometry factor, initial load, and crack length, respectively. In the case of single edge-crack semi-infinite elastic plate, the SIF was calculated as:

$$K = 2\sigma_0 \sqrt{a} \tag{3}$$

By investigating the case where  $\theta = 0$ , the maximum normal stress along the crack line becomes relevant. The distance  $r$  from the crack tip might be viewed as a characteristic length scale parameter in this case ( $r = \xi$ ). The stress concentration gets significantly immeasurable by approaching to the crack tip ( $\xi \rightarrow 0$ ). This behavior is an important feature of fracture



mechanics because it quantifies the stress concentration and importance of stress at the crack tip, which is crucial in predicting crack propagation and potential failure of materials and structures. Hence, the maximum stress component in the y-direction along the crack line in the framework of SIF will reduce to:

$$\sigma_y^{Max(SIF)} = 0.7979 \frac{\sqrt{a}}{\sqrt{\xi}} \sigma_0 \quad (4)$$

## FINITE ELEMENT ANALYSIS

Numerical simulation was conducted by considering the mechanical properties of an elastic plate using finite element modeling (FEM) in ABAQUS CAE software, as shown in Tab. 1. In this example, a two-dimensional elastic plate model with a width of 30 mm and a height of 50 mm is evaluated, as well as an initial tension stress of 1 MPa.

Items	Values	Units
Density $\rho$	7800	kg/m <sup>3</sup>
Elastic Modulus $E$	210000	MPa
Poisson's ratio $\nu$	0.3	-
Maximum principal stress	200	MPa
Initial tension $\sigma_0$	1	MPa
Width of plate $w$	50	mm
Height of plate $b$	30	mm

Table 1: Mechanical properties of model for numerical simulation.

The simulation included a wide variety of crack sizes ranging from ( $0 < a \leq 10$  mm), concerning a larger number of elements required for smaller crack sizes. Predefined cracks are present, but the particular crack path is unspecified. The simulation is carried out repeatedly with various crack lengths within the suggested range. To accomplish this, a local seeding strategy was implemented during the meshing process, which allowed for a higher element density near the crack without raising the element count for the entire model unduly. Furthermore, the numerical inquiry of crack analysis indicated meshing sensitivity [27], motivating the assessment of different mesh sizes, as illustrated in Tab. 2, to examine and analyze this phenomena.

Simulation iteration	Min - Max size of elements	Units
I	1.0 – 3.0	mm
II	0.5 – 1.0	mm
III	0.1 – 0.5	mm
IV	0.05 – 0.1	mm

Table 2: Different iterations of numerical simulation via ABAQUS CAE.

A detailed mesh sensitivity analysis was performed during the meshing process to evaluate the effect of altering mesh sizes on the outcomes. Four different simulations were performed, gradually improving the mesh from coarse to fine resolutions. The simulations were categorized as I, II, III, and IV, with mesh sizes ranging from 1.0 to 3.0 mm, 0.5 to 1.0 mm, 0.1 to 0.5 mm, and 0.05 to 0.1 mm, respectively. This method allows for a detailed investigation of the effect of mesh granularity on the outcomes, revealing insights into the susceptibility of the model to alternative meshing configurations. The elements that are considered to be 4-node bilinear plane stress quadrilateral, reduced integration, hourglass control (CPS4R). Fig 3 represents an example of an ABAQUS CAE software FEM simulation result for a normal stress distribution in the y-

direction. In this example, for simulation iteration II, the element size surrounding the crack is set to 0.5 mm, and the crack length is set to 7 mm. According to the analysis, the maximum normal stress in the y-direction is 5.80 MPa.

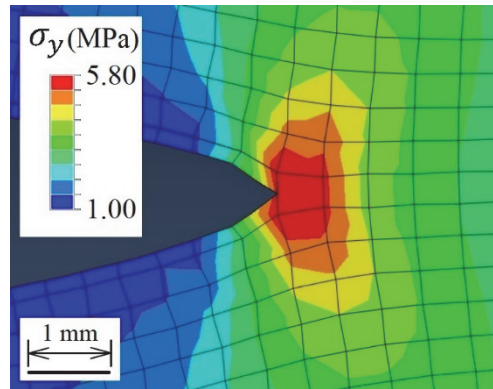


Figure 3: Normal stress distribution in the y-direction near the crack tip with simulation iteration II and crack length of 7 mm.

## MACHINE LEARNING MODEL

This part of the study discusses the application of algorithms for machine learning, particularly artificial neural network (ANN), for fracture analysis and maximum normal stress prediction. The predictions are based on numerical simulation data acquired from an edge-crack semi-infinite elastic plate fracture analysis. Additionally, the results are classified based on the different simulation iterations. The objective of implementing machine learning in this context is to create accurate and efficient model that is able to predict the maximum normal stress distribution around the crack tip, facilitating in the evaluation of fracture behavior and structural integrity.

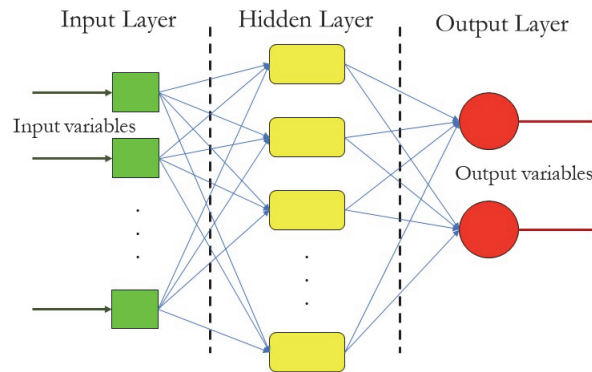


Figure 4: A generalized ANN structure with input to generating output based on the data processed by the input and hidden layers.

### *Artificial Neural Network (ANN)*

In the subject of fracture mechanics, the application of Artificial Neural Networks (ANN) along with Finite Element Analysis (FEA) has proven to be a valuable technique. FEA is widely employed in the engineering field developments to simulate and analyze complex fracture behavior and stress distribution. Engineers and researchers are able to employ machine learning to improve the accuracy and efficiency of fracture analysis by integrating ANN with FEA [28-30]. ANN can efficiently learn from massive amounts of data generated by FEA simulations, capturing complicated interactions between input parameters including material properties, crack geometry, loading and boundary conditions, and meshing types and the accompanying fracture responses [31,32]. This allows for more precise modeling of key crack propagation behavior, stress intensity factor, and stress distributions around the crack tip.

Fig 4 depicts a generalized ANN structure with input, hidden, and output layers. The first layer is the input layer, which accepts raw data or variables like crack length, mesh type, or initial load. The intermediary levels between the input and output layers are known as hidden layers. They are referred to as "hidden" since their activations are not readily visible or accessible. A hidden layer node gets input from the previous layer and creates an output. The number of hidden layers and neurons in each hidden layer can differ based on the complexity of the problem and the intended network performance.

Hidden layers are where the ANN receives and evaluates data patterns. This activation can be consider using the following equation.

$$A_i = \text{ReLU} \left( \sum_{j=1}^{n_{input}} W_{ij} x_j + B_i \right) \tag{5}$$

where  $A_i$  is the activation of neuron  $i$ ,  $W_{ij}$  is the weight of the connection between input neuron  $j$  and hidden neuron  $i$ ,  $x_j$  is the input feature  $j$ , and  $B_i$  is the bias of neuron  $i$ . Also, ReLU stands for the Rectified Linear Unit activation function.

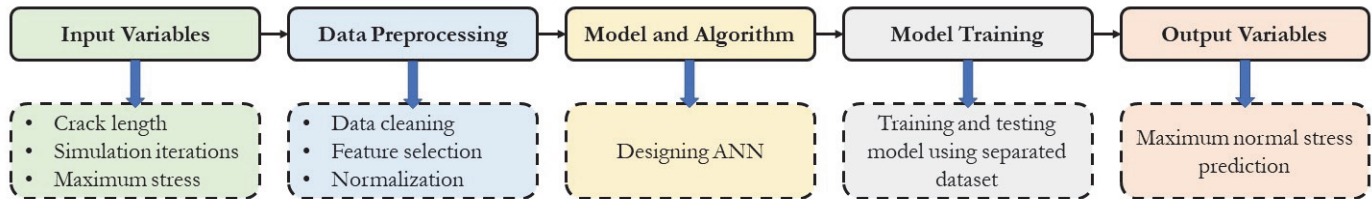


Figure 5: Flow chart of modeling ANN.

Crack length (mm)	Maximum normal stress in y-direction (MPa)							
	FEM				SIF			
	I	II	III	IV	$\xi = 1$	$\xi = 0.1$	$\xi = 0.05$	$\xi = 0.01$
0 <sup>+</sup>	1	1	1	1	0 <sup>+</sup>	0 <sup>+</sup>	0 <sup>+</sup>	0 <sup>+</sup>
1	1.15	1.70	1.90	3.42	0.80	2.52	3.57	7.98
2	1.30	2.30	3.06	5.85	1.13	3.57	5.05	11.28
3	1.46	3.00	4.19	8.00	1.38	4.37	6.18	13.82
4	1.61	3.60	5.02	10.70	1.59	5.05	7.14	15.96
5	1.76	4.45	6.05	13.11	1.78	5.64	7.98	17.84
6	1.91	5.10	7.28	15.40	1.95	6.18	8.74	19.54
7	2.07	5.80	8.10	18.10	2.11	6.67	9.44	21.11
8	2.22	6.50	9.10	20.00	2.26	7.14	10.09	22.56
9	2.38	7.43	10.35	22.30	2.39	7.57	10.70	23.94
10	2.52	8.10	11.30	25.30	2.52	7.98	11.28	25.23

Table 3: Numerical values of maximum normal stress in y-direction using FEM and SIF for different amounts of crack length.

The final layer is the output layer. It generates output based on the data processed by the input and hidden layers. The number of nodes in the output layer is determined by the scope of the problem. In binary classification problems, for example, one node may indicate the probability of belonging to one class, while another node represents the probability of belonging to the other. Fig 5 represents a conceptual illustration of an Artificial Neural Network (ANN) algorithms procedural designation. Beginning with the incorporation of relevant input variables such as crack length, simulation iterations, and maximum normal stress in the y-direction, the data is subjected to comprehensive data preprocessing techniques such as data modification, feature curation, and data normalization. Following that, the processed dataset is subjected to the required preparation for the implementation of the ANN algorithm. The resulting model is subjected to iterative training and validation phases using a separate dataset allocated for this purpose. Finally, the created model is capable of forecasting maximal normal stress based on FEM data.

The maximum normal stress in the y-direction for a semi-infinite elastic plate is represented numerically in Tab. 3. These values are obtained by FEM with different simulation iterations as well with SIF model. Various values of the characteristic length scale parameter are also included, depending on the amount of the crack length. Notably, these listed values provide the input dataset sent into the ANN algorithm, supplying both the testing and training stages of the model.

The algorithm of Tab. 4 gives a structured description of the stages in the Python code for predicting maximum normal stress with ANN. It begins with input and output breakdowns and then goes over each step of the procedure in detail.



Steps	Descriptions	Operations
Input	Excel file containing data	-
Output	Predicted maximum normal stress	-
1	Loading data	Load data from the Excel file using pandas.read_csv
2	Extract features and target	Extract input features (crack length, simulation iterations) and target output (maximum normal stress) from the loaded data.
3	Split dataset	Split the dataset into training and testing sets using train_test_split from sklearn.
4	Standardize features	Use StandardScaler from sklearn to standardize (normalize) the input features separately for training and testing sets. <ul style="list-style-type: none"> <li>• Create a sequential neural network model using tf.keras.Sequential from TensorFlow.</li> </ul>
5	Build ANN model	<ul style="list-style-type: none"> <li>• Add input layer with the number of input features and hidden layer with activation functions (ReLU).</li> <li>• Add an output layer with no activation for regression.</li> </ul>
6	Compile model	Compile the model using an optimizer ('adam') and a loss function ('mean_squared_error').
7	Train model	Train the model using model.fit with the standardized training data, specifying the number of epochs and batch size. <ul style="list-style-type: none"> <li>• Evaluate the trained model's performance on the standardized testing data using the evaluate method.</li> <li>• Calculate and display the test loss.</li> </ul>
8	Evaluate model	
9	Predict new data	Use the trained model to predict the maximum normal stress for the new data
10	Display results	Display the predicted maximum normal stress for the new data

Table 4: Algorithm of ANN for predicting maximum normal stress using Python programming.

As demonstrated in Tab. 4, the algorithm built to predict maximum normal stress adopts an ANN technique, which includes Rectified Linear Unit (ReLU) activation functions. The sequential approach starts by importing data from an Excel file, which includes variables such as crack length, mesh type, and maximum normal stress, as well as a possibility for new data for prediction actions. Following the extraction of relevant characteristics and target output from the obtained dataset, the algorithm partitions the dataset into discrete training and testing subsets. Preceding to model development within the TensorFlow framework, as a predefined library for ANN, attributes are standardized for corresponding scales. In this case, a feed forwarded neural network with 64 neurons and ReLU activation in the input layer, 32 neurons and ReLU activation in the hidden layer, and 1 neuron in the output layer is utilized. Following preparation via an optimizer and loss function, the model is trained using standardized training data. The performance of the model is extensively checked on the testing dataset after training. Additionally, predictive capabilities extend to unique data instances in which inputs are scaled in accordance with training procedures, resulting in predicted maximum normal stress values. However, the method ends by showing predicted maximum normal stress outputs while also reflecting the efficacy of the model employing key metrics such as Mean Absolute Error (MAE), Root Mean Square Error (RMSE), and the R-squared coefficient ( $R^2$ ). The Python code is provided in the full form in the Appendix at the end of the paper.

## RESULTS AND DISCUSSION

The comparison and description of the results obtained for the maximum normal stress from the SIF model and the FEM simulation has been performed in this section. In Fig 6, four distinct characteristic length values (0.01, 0.05, 0.1, and 1.0 mm) are utilized in the SIF model, while the simulation extracts the maximum stress values for different crack lengths using particular simulation iterations. Fig 6 displays that the finite element modeling has no perceptible effect of the characteristic length scale, with stress increasing linearly as the crack length increases. Furthermore, the mesh dependency of the FEM results is recognizable, with similar outcomes for decreasing characteristic length sizes as element size declines.

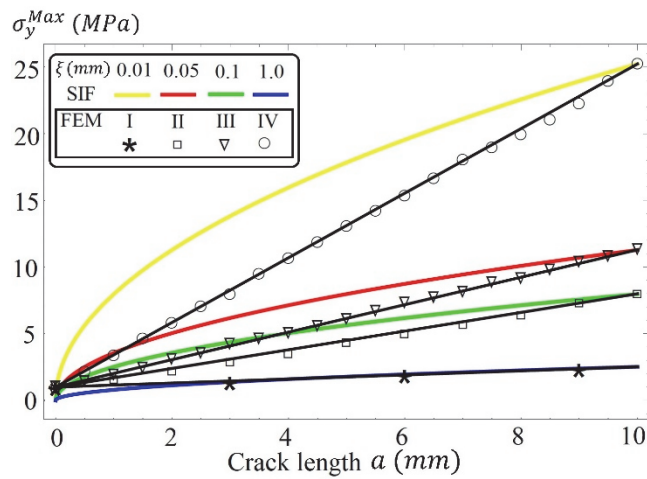


Figure 6: Comparison of maximum normal stress in y-direction of SIF model and FEM for different amount of crack length.

In addition, Fig 7 investigates the effect of crack length on the maximum stress component in the y-direction estimated from the SIF model over a range of characteristic lengths ( $0 < \xi \leq 1$  mm). Notably, as illustrated in Fig 7, reaching the exact crack tip ( $\xi = 0$ ) is impractical due to stress concentration, which results in an infinite maximum stress value. The simulation data for the four distinct crack lengths (0.1, 1.0, 5.0, and 10 mm) are depicted on the relevant crack length curves. Assuming implementing simulation iteration II, for example, the red curve displaying a crack length of 5.0 mm corresponds to a maximum stress value of 4.5 MPa when the characteristic length is 0.16 mm, matching the SIF model result.

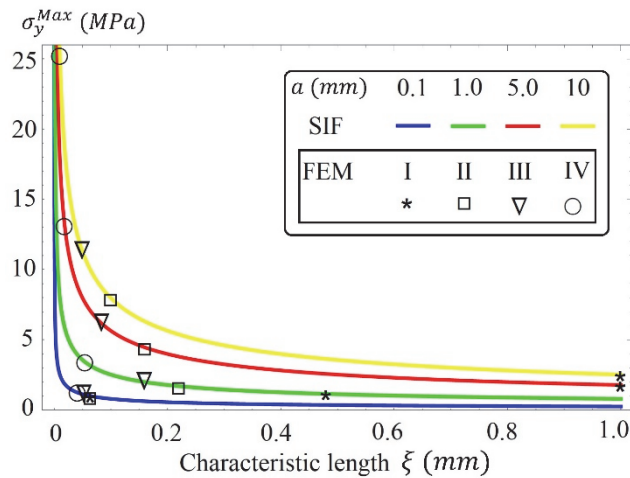


Figure 7: Comparison of maximum normal stress in y-direction of SIF model and FEM for different amount of characteristic length.

The outputs of the ANN model are discussed as well here. Tab. 5 provides the data that was elected as test data for ANN prediction.

In this study, 10% of the total dataset obtained from simulations has been set apart for testing, guaranteeing that these specific data points were not exposed to the ANN model during the training phase. The results of the ANN for this specific testing dataset are considered predictions from the machine learning model. The procedure is illustrated in Tab. 5, where the ANN model predicts data that has not before been seen during the training phase. For instance, the ANN model predicts a result of 1.18 MPa when the FEM yields 1.15 MPa for a crack length of 1 mm in the first simulation iteration, demonstrating high accuracy of machine learning model. An important part of assessing the performance of machine learning model is the selected test data. As these test data points are distinct from the training dataset, the model is subjected to the circumstances that it was not trained on. This deliberate omission benefits to evaluate the capacity of the model for generalization and precise prediction-making on fresh, untested data. By essentially subjecting the machine learning model to various situations, it is possible to evaluate its ability to predict and obtain insight into its general reliability and efficacy.





Crack Length (mm)	Simulation iteration	Maximum normal stress (MPa)		Error (%)
		FEM	ANN	
1	I	1.15	1.18	2.54
2	II	2.30	2.26	1.77
3	I	1.46	1.40	4.28
3	II	3.00	2.95	1.69
4	I	1.61	1.74	7.47

Table 5: Selected data for prediction in ANN model.

Moreover, Tab. 6 serves as a valuable point of reference, providing a comprehensive assessment of the performance of ANN model based on the evaluative test dataset provided in Tab. 5 and the remaining 90% of data utilized for model training. This detailed review is based on a wide range of performance criteria that have been rigorously used to measure the algorithms accuracy and precision. The metrics used specifically include the R-squared coefficient ( $R^2$ ), which represents the proportion of variation captured by the model, as well as the mean absolute error (MAE) and root mean square error (RMSE), two important indicators quantifying the predictive discrepancy and spread of model, respectively.

Model Performance Metric	Testing data	Training data
$R^2$	0.978	0.999
MAE	0.090	0.107
RMSE	0.098	0.157

Table 6: ANN model performance.

The observed ML model performs well according to the already established criteria, as seen by the values assigned to  $R^2$  (0.978 and 0.999), MAE (0.090 and 0.107), and, RMSE (0.098 and 0.157) for testing data and training data, respectively. Tab. 6 compacts this presentation of statistical facts and performance indicators, boosting confidence and understanding of the predictive potential of ANN model in the context of the test dataset.

Notable advances are introduced when ANN is used in the fields of fracture mechanics and FEM. The creation of prediction models using data from simulations is streamlined by the use of ANN. After going through a thorough validation procedure and evaluating ANN performance, these models might be used instead of direct FEM simulations. In the context of the study that is being reported, this shift denotes a significant gain in computing efficiency and prediction accuracy. In addition to improving the creation of precise predictive models, the work signifies a paradigm change in the direction of more effective simulation-based predictions in engineering and materials science by utilizing the capabilities of ANN.

## CONCLUSION

In conclusion, the stress intensity factor (SIF) model was used to develop and analyze the maximum normal stress formulation within a semi-infinite edge-crack elastic plate, and its correspondence with finite element method (FEM) results was thoroughly investigated across a range of distinct crack lengths. The inherent influence of the characteristic length parameter has also been carefully considered. Notably, the FEM-derived results laid the framework for the development of a predictive model using a machine learning (ML) technique. Several key observations appear from these endeavors:

- In the context of the SIF model, a decrease in the characteristic length parameter corresponds to a closer proximity to the crack tip, revealing the significant influence of stress concentration. The pursuit of exact FEM analysis for this purpose necessitates a reduction in element size or an increase in the number of elements, albeit at the consequence of increased simulation costs.
- The incorporation of ML approaches simplifies the development of prediction models based on simulation-derived data. Following a rigorous validation process and a thorough assessment of ML performance, this model may provide an alternative to direct FEM simulations, representing a significant advancement in computational efficiency and predictive accuracy within the context of the presented study.



- It is worth noting the significant effect of element size on results, particularly in the setting of critical fracture propagation stress when using the energy criteria. While inconsequential for AAN training or assessment, this impact lacks the acquired outcomes of physical meaning.

## ACKNOWLEDGEMENTS

**F**undamental Research Grant Scheme Ministry of Higher Education Malaysia under Institution of Universiti Kebangsaan Malaysia (UKM) funded this research, grant number: FRGS/1/2022/TK10/UKM/02/30.

## APPENDIX

Python code of ANN algorithm:

```
import pandas as pd
import numpy as np
import tensorflow as tf
from sklearn.model_selection import train_test_split
from sklearn.preprocessing import StandardScaler
from sklearn.metrics import mean_absolute_error, mean_squared_error, r2_score
data = pd.read_csv('file.csv')
X = data[['Crack_Length', 'Simulation_Iteration']]
y = data['Maximum_Normal_Stress']
X_train, X_test, y_train, y_test = train_test_split(X, y, test_size=0.1, random_state=42)
scaler = StandardScaler()
X_train_scaled = scaler.fit_transform(X_train)
X_test_scaled = scaler.transform(X_test)
model = tf.keras.Sequential([
    tf.keras.layers.Dense(64, activation='relu', input_shape=(X_train_scaled.shape[1],)),
    tf.keras.layers.Dense(32, activation='relu'),
    tf.keras.layers.Dense(1) # Output layer
])
model.compile(optimizer='adam', loss='mean_squared_error')
model.fit(X_train_scaled, y_train, epochs=500, batch_size=32, validation_split=0.1)
loss = model.evaluate(X_test_scaled, y_test)
predicted_stress = model.predict(X_test_scaled)
y_pred = model.predict(X_test_scaled)
mae = mean_absolute_error(y_test, y_pred)
rmse = np.sqrt(mean_squared_error(y_test, y_pred))
r2 = r2_score(y_test, y_pred)
print("Predicted Maximum Normal Stress:", predicted_stress)
print("Mean Absolute Error:", mae)
print("Root Mean Square Error:", rmse)
print("R-squared:", r2)
```

## REFERENCES

- [1] Moghtaderi, S.H., Faghidian, S.A., Shodja, H.M. (2018). Analytical determination of shear correction factor for Timoshenko beam model, *Steel and Composite Structures*, 29(4), pp. 483–491. DOI: 10.12989/scs.2018.29.4.483.
- [2] Fazlali, M., Moghtaderi, S.H., Faghidian, S.A. (2021). Nonlinear flexure mechanics of beams: Stress gradient and nonlocal integral theory, *Mater Res Express*, 8(3). DOI: 10.1088/2053-1591/abe3c6.



- [3] Konieczny, M.M., Achtehik, H., Gasiak, G. (2021). Influence of the applied layer on the state of stress in a bimetallic perforated plate under two load variants, *Frattura Ed Integrita Strutturale*, 15(56), pp. 137–150. DOI: 10.3221/IGF-ESIS.56.11.
- [4] Kenanda, M.A., Hammadi, F., Belabed, Z., Hadj Meliani, M. (2023). Free vibration analysis of the structural integrity on the porous functionally graded plates using a novel Quasi-3D hyperbolic high order shear deformation theory, *Frattura Ed Integrità Strutturale*, 17(64), pp. 266–282. DOI: 10.3221/IGF-ESIS.64.18.
- [5] Faghidian, S.A., Mohammad-Sedighi, H. (2022). Dynamics of nonlocal thick nano-bars, *Eng Comput*, 38(3), pp. 2487–2496. DOI: 10.1007/s00366-020-01216-3.
- [6] Moghtaderi, S.H., Faghidian, S.A., Asghari, M. (2023). Nonlinear vibrations of gradient and nonlocal elastic nano-bars, *Mechanics Based Design of Structures and Machines*, 51(3), pp. 1316–1334. DOI: 10.1080/15397734.2020.1864640.
- [7] Moghtaderi, S.H., Jedi, A., Ariffin, A.K. (2023). A Review on Nonlocal Theories in Fatigue Assessment of Solids, *Materials*. DOI: 10.3390/ma16020831.
- [8] Samir Mohamed Mohamed Soliman, E. (2021). Mode I stress intensity factor with various crack types, *Frattura Ed Integrità Strutturale*, 16(59), pp. 471–485. DOI: 10.3221/IGF-ESIS.59.31.
- [9] Fischer, C., Fricke, W. (2015). Influence of local stress concentrations on the crack propagation in complex welded components, *Frattura Ed Integrita Strutturale*, 9(34), pp. 99–108. DOI: 10.3221/IGF-ESIS.34.10.
- [10] Nowak, K. (2015). Paths of interactive cracks in creep conditions, *Frattura Ed Integrita Strutturale*, 9(34), pp. 507–514. DOI: 10.3221/IGF-ESIS.34.56.
- [11] Salvati, E., Livieri, P., Tovo, R. (2013). Mode I Stress Intensity Factors for triangular corner crack nearby intersecting of cylindrical holes, *Frattura Ed Integrita Strutturale*, 26, pp. 80–91. DOI: 10.3221/igf-esis.26.09.
- [12] Alebrahim, R., Thamburaja, P., Srinivasa, A., Reddy, J.N. (2023). A robust Moore–Penrose pseudoinverse-based static finite-element solver for simulating non-local fracture in solids, *Comput Methods Appl Mech Eng*, 403. DOI: 10.1016/j.cma.2022.115727.
- [13] Shin, H.Y., Thamburaja, P., Srinivasa, A.R., Reddy, J.N. (2023). Modeling impact fracture in a quasi-brittle solids using a 3D nonlocal graph-based finite element analysis: Theory, finite element simulations, and experimental verification, *J Mech Phys Solids*, 170, p. 105097. DOI: 10.1016/j.jmps.2022.105097.
- [14] Kamaludin, S., Thamburaja, P. (2023). Efficient Neighbour Search Algorithm for Nonlocal-Based Simulations—Application to Failure Mechanics, *Journal of Failure Analysis and Prevention*, 23(2), pp. 540–547. DOI: 10.1007/s11668-023-01602-1
- [15] Le-Ngoc, V., Vuong Cong, L., Pham Bao, T., Ngo Kieu, N. (2023). Damage assessment in beam-like structures by correlation of spectrum using machine learning, *Frattura Ed Integrità Strutturale*, 17(65), pp. 300–319. DOI: 10.3221/igf-esis.65.20.
- [16] Kamble, A., He, S., Howse, J.R., Ward, C., Hamerton, I. (2023). Exploiting the use of deep learning techniques to identify phase separation in self-assembled microstructures with localized graphene domains in epoxy blends, *Comput Mater Sci*, 229. DOI: 10.1016/j.commatsci.2023.112374.
- [17] Arbaoui, A., Ouahabi, A., Jacques, S., Hamiane, M. (2021). Wavelet-based multiresolution analysis coupled with deep learning to efficiently monitor cracks in concrete, *Frattura Ed Integrita Strutturale*, 15(58), pp. 33–47. DOI: 10.3221/IGF-ESIS.58.03.
- [18] Liu, X., Athanasiou, C.E., Padture, N.P., Sheldon, B.W., Gao, H. (2020). A machine learning approach to fracture mechanics problems, *Acta Mater*, 190, pp. 105–112. DOI: 10.1016/j.actamat.2020.03.016.
- [19] Nguyen, T.H., Vu, A.T. (2021). Evaluating structural safety of trusses using machine learning, *Frattura Ed Integrita Strutturale*, 15(58), pp. 308–318. DOI: 10.3221/IGF-ESIS.58.23.
- [20] Mishra, A., Vats, A. (2021). Supervised machine learning classification algorithms for detection of fracture location in dissimilar friction stir welded joints, *Frattura Ed Integrita Strutturale*, 15(58), pp. 242–253. DOI: 10.3221/IGF-ESIS.58.18.
- [21] Ince, R. (2010). Artificial neural network-based analysis of effective crack model in concrete fracture, *Fatigue Fract Eng Mater Struct*, 33(9), pp. 595–606. DOI: 10.1111/j.1460-2695.2010.01469.x.
- [22] Bui-Ngoc, D., Nguyen-Tran, H., Nguyen-Ngoc, L., Tran-Ngoc, H., Bui-Tien, T., Tran-Viet, H. (2022). Damage detection in structural health monitoring using hybrid convolution neural network and recurrent neural network, *Frattura Ed Integrita Strutturale*, 16(59), pp. 461–470. DOI: 10.3221/IGF-ESIS.59.30.
- [23] Alipour, M., Esatyana, E., Sakhaee-Pour, A., Sadooni, F.N., Al-Kuwari, H.A. (2021). Characterizing fracture toughness using machine learning, *J Pet Sci Eng*, 200, p. 108202. DOI: 10.1016/j.petrol.2020.108202.
- [24] Moore, B.A., Rougier, E., O'Malley, D., Srinivasan, G., Hunter, A., Viswanathan, H. (2018). Predictive modeling of dynamic fracture growth in brittle materials with machine learning, *Comput Mater Sci*, 148, pp. 46–53.



- DOI: 10.1016/j.commsci.2018.01.056.
- [25] Mahmoodzadeh, A., Fakhri, D., Hussein Mohammed, A., Salih Mohammed, A., Hashim Ibrahim, H., Rashidi, S. (2023). Estimating the effective fracture toughness of a variety of materials using several machine learning models, *Eng Fract Mech*, 286, p. 109321. DOI: 10.1016/j.engfracmech.2023.109321.
- [26] Stephens, R. I., Fatemi, A., Stephens, R. R. and Fuchs, H. O. (2000). *Metal fatigue in engineering*, New York, John Wiley & Sons.
- [27] Thamburaja, P., Sarah, K., Srinivasa, A., Reddy, J.N. (2019). Fracture of viscoelastic materials: FEM implementation of a non-local & rate form-based finite-deformation constitutive theory, *Comput Methods Appl Mech Eng*, 354, pp. 871–903. DOI: 10.1016/j.cma.2019.05.032.
- [28] Khoei, A.R., Moslemi, H., Seddighian, M.R. (2020). An efficient stress recovery technique in adaptive finite element method using artificial neural network, *Eng Fract Mech*, 237. DOI: 10.1016/j.engfracmech.2020.107231.
- [29] van de Weg, B.P., Greve, L., Andres, M., Eller, T.K., Rosic, B. (2021). Neural network-based surrogate model for a bifurcating structural fracture response, *Eng Fract Mech*, 241. DOI: 10.1016/j.engfracmech.2020.107424.
- [30] Badarinath, P.V., Chierichetti, M., Kakhki, F.D. (2021). A machine learning approach as a surrogate for a finite element analysis: Status of research and application to one dimensional systems, *Sensors*, 21(5), pp. 1–18. DOI: 10.3390/s21051654.
- [31] Nasir, T., Asmael, Mohammed., Zeeshan, Q., Solyali, D. (2020). Applications of Machine Learning to Friction Stir Welding Process Optimization, *Jurnal Kejuruteraan*, 32(2), pp. 171–186. DOI: 10.17576/jkukm-2020-32(2)-01.
- [32] Long, X.Y., Zhao, S.K., Jiang, C., Li, W.P., Liu, C.H. (2021). Deep learning-based planar crack damage evaluation using convolutional neural networks, *Eng Fract Mech*, 246. DOI: 10.1016/j.engfracmech.2021.107604.